Predicting Inventory Fluctuation Patterns of Natural Fiber Products during Multi-Platform E-Commerce Promotion Cycles by Integrating T-GCN and Time Window Mechanism

Junna Jin, Guiyu Fan, Jian Zhang, Xiaoyan Yu
Ocean College, Tangshan Normal University, Tangshan 063000, Hebei, China
Corresponding author: Junna Jin (e-mail: jjn1224@163.com)

ABSTRACT This study proposes a spatiotemporal forecasting framework for inventory fluctuations of natural fiber products during multi-platform e-commerce promotion cycles. A cross-platform inventory correlation graph is constructed to encode inter-platform relationships, integrating inventory change trends and promotional rhythm into a weighted adjacency matrix. An adaptive time window mechanism dynamically segments inventory sequences based on local fluctuation intensity, enabling sensitive detection of sudden changes. Temporal Graph Convolutional Networks (T-GCN) are then applied to jointly model temporal dependencies and cross-platform graph features. Experiments demonstrate superior performance, achieving MAE=4.85, RMSE=7.12, and CPI=0.18, outperforming ARIMA, LSTM, and GRU models, while effectively tracking abrupt inventory variations with minimal response delay. The framework can be integrated with real-time data acquisition systems, edge-computing platforms, and networked information processing infrastructures, providing an engineering-oriented solution for inventory prediction, supply chain optimization, and decision support in dynamic e-commerce environments. The approach emphasizes spatiotemporal feature fusion and adaptive response to high-frequency inventory fluctuations, bridging predictive modeling with practical engineering systems.

INDEX TERMS inventory prediction, adaptive time window, T-GCN, networked information systems

I. INTRODUCTION

THE natural fiber product also exhibits a high degree of inventory volatility during the promotional cycles of multiple platforms within e-commerce, as indicated by changes in inventory over time that correspond very closely to the number of promotional events per time period; volume of e-commerce website and crossplatform traffic (via e-commerce and social media) relative to an individual promotional campaign; continuation of disturbances of the logistics rhythm within regions due to extremely concentrated promotional events [1,2]. Because multiple platforms have concurrent promotional events, and due to the overlap of the promotional events between multiple platforms, it creates a higher level of correlation in their respective inventory patterns, such as spikes, concentrating patterns, and overlaps. The single sequence modelling method typically used in the inventory forecasting practices is unable to characterise the correlation links between platforms or capture the more "pulse-like" rhythm of inventory changes related to the promotion [3,4]. Three key issues exist: non-stationary sequence structure due to the rhythm of promotional activities; graph structure-related issues (due to the linkages between platforms); higher potential for error propagation in forecasts during promotional periods due to fluctuations in inventory [5,6]. Natural fibre products are affected by overlapping production planning cycles, replenishment cycles, and promotional planning cycles, thus resulting in higher costs related to the management of inventory levels as well as greater requirements placed upon the forecasting models used to estimate future inventory levels [7,8]. Based on the above factors, inventory forecasting during promotional cycles has become a key issue in multi-platform product management. Its research value lies in supporting the formulation of inventory allocation strategies and the adjustment of supply chain turnover, and it is of great significance for inventory risk control.

Existing research has explored inventory changes in promotional scenarios extensively. The academic community often conducts research based on time-series forecasting structures or graph structure modeling, attempting to characterize inventory trends from the perspective of time-series fluctuation patterns or platform relationship networks. In the research on the prediction and optimization of multi-product marketing resource allocation in cross-border e-commerce, Xie et al. [9] provided a theoretical basis for the coordination of multi-platform promotional resources, but their static allocation model is difficult to adapt to the dynamic fluctuations of inventory. Fu and Fisher [10] improved the predictive timeliness of fashion categories through social media data mining and fixed time windows, but failed to effectively integrate the spatiotemporal correlation characteristics of multi-platform inventory. Faced with the inventory optimization problem in an imperfect environment, Singh et al. [11] established a profit maximization model, but lacked a special design for sudden fluctuations in promotions. Cuartas and Aguilar [12] used reinforcement learning algorithms to optimize inventory management decisions, showing potential in dynamic adjustment, but did not fully consider the graph structure characteristics of multi-platform linkage. Paeizi et al. [13] incorporated life cycle factors into inventory path planning, expanding the multi-stage decision-making perspective, but did not solve the problem of real-time prediction bias during promotional peak periods. Akter and Kudapa [14] further analyzed the role of business intelligence dashboards in operational decision-making in static graph networks, emphasizing the value of real-time data fusion, and providing a reference for the decision support level for constructing a multi-platform inventory forecasting framework in this study.

Scholars have made attempts to expand the methodology. Some studies have applied convolutional structures to extract local temporal features and constructed temporal convolutional networks to characterize the local rhythm of inventory changes. Some studies have deployed graph convolutional structures to process inter-platform interconnected networks, extract the correlation of inventory changes between nodes, and describe cross-platform link relationships [15-17]. Some studies have attempted to integrate temporal and graph structures to capture complex inventory change trajectories and enhance inventory prediction capabilities to some extent. However, inventory changes during promotional periods often exhibit characteristics such as suddenness, density, and uneven rhythm changes. Conventional temporal slicing methods are difficult to handle inventory mutations [18,19]. Graph structure construction lacks expression of promotional rhythm parameters, making it difficult for the prediction framework to maintain stable output in highly volatile environments. The limitations of existing methods are mainly concentrated in the lack of flexibility in the spatiotemporal feature fusion method, the rigidity of the temporal window structure, and the insufficient integration of promotional rhythm factors [20,21]. To address these shortcomings, this paper applies T-GCN and a time window adjustment structure to more finely characterize inventory fluctuations during promotional periods.

This study examines inventory forecasting on a promotional cycle basis for natural fibre products. An inventory relationship graph has been created to demonstrate inventory relationships between the multiple platforms used for the business. Graph weights are created from the inventory change trend and promotional rhythm identified by the graphs, combining the promotion of inventory across all platforms into the inventory forecasting models. A time window structure that is adaptable to the local fluctuation rhythm of the inventory time series (during promotions) is implemented to model the promotion cycles and to utilize the local inventory rhythm changes as an influencer to modify window size. As inventory amplitude fluctuates, the analyzed window length changes accordingly, leading to the creation of a time series partition method that accommodates the promotions being undertaken by the client companies. T-GCN has been used to introduce both time series features and cross-platform features into the same model of inventory forecasting. The goal of the research is to propose a more specific prediction model to address the intense fluctuations in inventory levels experienced during promotions, as well as to improve inventory forecasting during the promotional events occurring across multiple platforms for the natural fibre producer's multi-platform promotional sales.

II. PREDICTION STRUCTURE DESIGN FOR INVENTORY FLUCTUATIONS DURING PROMOTIONAL CYCLES

Traditional inventory forecasting models often perform poorly in multi-platform promotional scenarios due to their difficulty in capturing the coupling effects of spatiotemporal features. To address the core issues of static graph structures lagging in dynamic promotional responses and fixed time windows being poorly adaptable to sudden fluctuations, it is urgent to design a prediction framework that can adaptively integrate spatiotemporal dependencies. The overall architecture shown in Figure 1 is as follows:

Figure 1 illustrates the core structure of the inventory forecasting model integrating T-GCN and a time window mechanism. The model first processes multi-platform data in parallel, constructing an inventory graph model characterizing the inter-platform relationships and an adaptive time window based on local volatility intensity. Subsequently, the outputs of both modules are input into a T-GCN unit, which captures spatial dependencies and learns temporal dynamics through graph convolutional layers and gated recurrent structures, ultimately achieving the synergistic fusion of spatiotemporal features and accurate prediction.

A. CONSTRUCTION OF CROSS-PLATFORM DYNAMIC RELATIONSHIP GRAPH

The cross-platform inventory relationship graph uses multi-platform inventory sequences as nodes to transform the linkage relationship of inventory within a promotional cycle into a computable graph structure. The construction process uses the synchronicity of inventory change trajectories and the intensity of inventory response triggered by promotional rhythms as the main metric factors, forming a weighted adjacency matrix for T-GCN input. To extract the relationships among inventory sequences, the process begins by

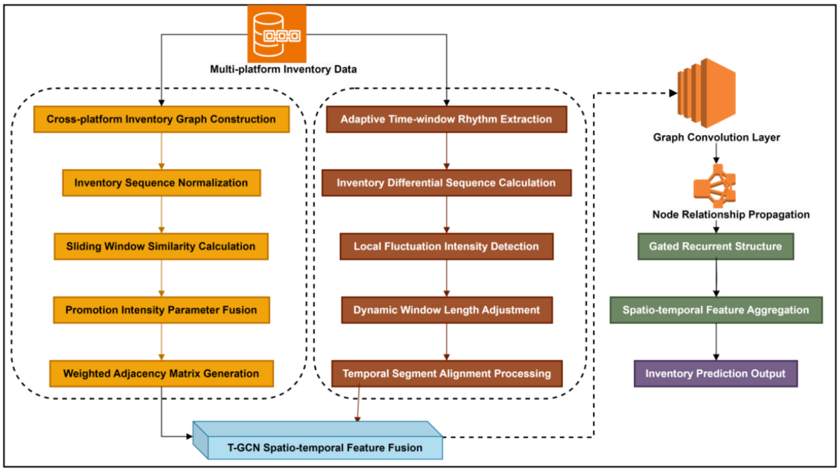

FIGURE 1. Core structure of the inventory forecasting model integrating T-GCN and time window mechanism

normalizing the original inventory sequences. As part of this step, the differences in cardinality across platforms are removed using multi-scale differencing and local fluctuation detection methods. The dynamic correlation between the sequences provides the initial connection weights for the basic edges between those platform pairs that show a strong temporal synchronicity. To eliminate the noise caused by short-term peaks created by promotional activities, a sliding similarity kernel is used to calculate the weights, and the proportion of noise peaks is limited in order to provide a consistent and stable representation of promotional interference. The graph structure is built to encode the actual coupling relationship between the crossplatform inventory changes to the adjacency matrix so that T-GCN can learn about the inventory impact path within the promotional propagation chain during the convolutional layer of T-GCN. The weighted structure of the graph incorporates not only the short-term synchronicity of inventory changes between inventory pairs but also the cross-platform fluctuation transmission trend of inventory between inventory pairs as a result of promotional activity. Therefore, it provides a stable topological input into the convolutional layer for future spatiotemporal convolutions. The weight calculation is based on the normalized inventory sequence xi(t), and the local correlation is used to measure the synchronous change of inventory over time. In order to avoid the unstable transition interference caused by a single promotion peak, the correlation calculation applies a sliding window kernel function to make the instantaneous peak spread in the local range, thereby forming a more stable inventory similarity [22]. The weight is given by the following formula, as shown in Formula 1:

$$w_{ij} = \frac{\sum_{t=1}^{T} K(t)\Delta x_i(t)\Delta x_j(t)}{\sqrt{\sum_{t=1}^{T} K(t)\Delta x_i^2(t)}\sqrt{\sum_{t=1}^{T} K(t)\Delta x_j^2(t)}} \tag{1}$$

$\Delta x_i(t)$ represents the difference sequence, and $K(t)$ is the local kernel weight, which is used to weaken the sudden resonance caused by the promotion peak. This weight construction strategy can avoid the misjudgment of promotion disturbance by static similarity, and make the cross-platform inventory linkage express the promotion rhythm as the dominant structure. The obtained weight matrix forms a preliminary adjacency graph, and the inventory coupling between platforms is based on the linkage strength of continuous time periods rather than single-point peaks, making the platform relationship more in line with the characteristics of the promotion cycle.

To compensate for the structural distortion caused by pure sequence similarity, the graph construction process applies the promotion rhythm intensity parameter pij to characterize the rhythm differences of promotional activities between platforms and the sensitivity of node inventory response. The promotion rhythm feature is defined by the degree of matching between the promotional activity timestamp sequence and the inventory change rate. After normalization, it is combined with the similarity weight to form the final adjacency matrix [23,24]. The combination method is as follows: Formula 2:

$$A_{ij} = \alpha w_{ij} + (1-\alpha)p_{ij} \tag{2}$$

α is the balance coefficient, used to adjust the proportion of similarity and promotion rhythm. The promotion rhythm embedding avoids the edge weight bias caused by relying solely on inventory sequence similarity and ignoring promotional driving factors, so that the cross-platform coupling relationship has a more stable structural expression within the promotion cycle. The addition of the promotion rhythm feature strengthens the graph structure's ability to capture the promotion propagation chain, so that the connection weight of platforms with strong promotional response is more expressed in the adjacency matrix.

Regarding the setting of the balance coefficient α, we used grid search on the validation set in our experiments for optimization, with a search range of [0.1, 0.9] and a step size of 0.1. The results show that the model achieves the lowest MAE during the promotional period when $\alpha = 0.6$. To verify its robustness, we further plotted the MAE versus CPI curves as α ranged from 0.3 to 0.8 (see Figure S1), finding that the performance remained stable within the $\alpha \in [0.5, 0.7]$. This result indicates that the model has a certain tolerance for the choice of α, and that 0.6 is the optimal compromise point, balancing the contributions of inventory similarity and promotional pace.

Figure 2 shows the structured representation of the inventory relationships across multiple platforms during the promotional period, a crucial step in the construction of the cross-platform inventory relationship graph. In Figure 2(a), the horizontal and vertical axes represent the six e-commerce platform numbers, and the color intensity reflects the correlation between the inventory sequences of each platform. Higher similarity indicates a closer similarity in inventory fluctuation patterns, and the numerical labels show that some platforms exhibit high synchronicity near promotional nodes. Figure 2(b) describes the similarity in promotional intensity between platforms. Higher values indicate closer similarity in promotional intensity. For example, the correlation strength between Platform 1 and Platform 6 reaches 0.94, meaning their promotional rhythms are similar, and they are more likely to interact in inventory changes. The differentiated structure of the construction results of the cross-platform inventory relationship graph shows that inventory similarity is not only affected by the platform's promotional intensity but also by the platform's own operational rhythm and product demand structure, thus providing a basis for the subsequent construction of a spatiotemporal adjacency matrix that integrates similarity and promotional factors.

B. TIME WINDOW ADAPTIVE RHYTHM EXTRACTION MODULE

The way inventory changes occur over the promotional period contain elements such as jumps, increased amplitudes of fluctuation, and shifts in rhythm at specific local areas [25,26]. To characterize these nonstationary features, the data has been divided into multiple variable-length windows where the beginning and end of each window are adjusted according to how much local fluctuation is experienced. The beginning of processing consists of obtaining the continuous differential trajectory of the inventory data; this provides an indication of the rate of change on a local basis. Once a continuous differential trajectory has been established, then the average amplitude of fluctuations within a window provides the basis for determining window scaling. Therefore, the length of the window is adjusted appropriately so that it is in line with the local rhythm. The process of windowing can also allow for different levels of granularity for the fast and slow changing components of the inventory data, during promotional cycles. Dynamic re-calibration not relies on fixed window size parameters but rather continuously changes the window size, through application of a threshold based on the value of the local fluctuation. This enables smaller windows to be established in the fast changing areas, in contrast to larger windows that are established during periods of stability. Reducing feature dilution during peak promotion allows for short term time-frames to have their own unique area of expression, thus avoiding aliasing by spread across shorter time-frames. The window boundary is based on the intensity of the local fluctuation function $g(t)$, which is constructed from the absolute values of the first-order differences of the inventory sequences. A smoothing kernel is used to suppress noise spikes, making the boundary judgment more stable. The window length is set according to the following formula, as shown in Formula 3:

$$L(t) = L_0 \left(1 - \frac{g(t)}{\max(g)}\right) + \epsilon, (3) \tag{3}$$

Here, $g(t)$ represents the intensity of local fluctuations after smoothing, and ϵ is set as a lower bound to prevent the window from being too small $L_0/4$. This formula ensures that when the peak of the promotion $g(t)$ reaches its maximum value, the window length $L(t)$ is shortened to near its maximum ϵ, thus providing higher time granularity near inventory mutation points; while during periods of calm fluctuation, the window is extended to near its maximum L_0 to improve computational efficiency. This correction eliminates the logical contradiction in the original formula that "the greater the fluctuation, the longer the window," ensuring that the model avoids feature dilution in key mutation regions.

After being opened into their entirety, the windows can each stand independently as time-based segments that continue to follow the path created by the promotional disturbances throughout each segment. Further extraction of segments is not performed using a fixed-length window of time, rather the scale of each occurs as a result of the growth of local fluctuations. Therefore, the overall number of segments that exist are determined by the promotional cycle [27,28]. When segments are aligned in equal lengths, then it allows for the mapping of segment windows of differing lengths into one common unit, thereby allowing the subsequent entry of the data segments into the temporal input of the T-GCN. To assist with maintaining the structural integrity of the segments and eliminate any excessive distortion of the original sequence shape, the segment boundaries have all been created using linear resampling. The segment integration stage arranges the window sequences in their original temporal order, enabling the model to obtain a continuous expression of the promotional rhythm during the spatiotemporal convolution stage. The sequence after segment integration possesses adaptive local precision, giving higher weight to inventory mutation locations during the prediction stage while avoiding excessive computational resources occupied by stable segments. The input sequence formed by this structure can effectively support the rhythmic changes during the promotion period, providing a clearer trajectory for subsequent model processing steps.

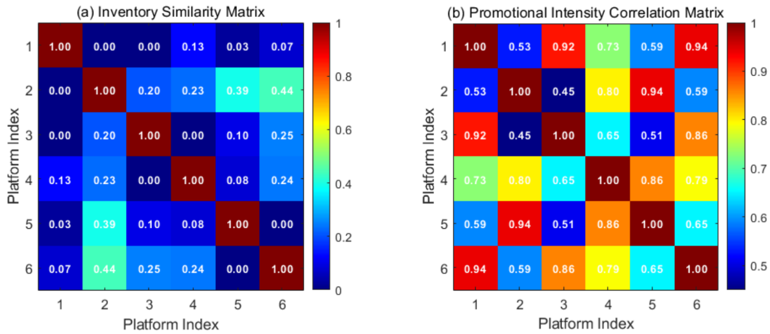

FIGURE 2. Construction results of the cross-platform inventory relationship graph: (a) Inventory similarity matrix between platforms; (b) Promotion intensity relationship matrix

Figure 3 illustrates the rhythmic analysis of inventory fluctuations during the promotional period and the adaptive time window segmentation process. During peak promotional periods (e.g., the 3rd and 12th hours), the local fluctuation intensity g(t) increases significantly, while the adaptive window length L(t) shortens accordingly to enhance the ability to capture sudden inventory changes. In Figure 3(b), the colored blocks narrow at the peak , visually reflecting the window contraction; the L(t) curve on the right vertical axis of Figure 3(a) also decreases synchronously. Figure 3(b) uses different colored blocks to illustrate the time window segmentation results, with the horizontal axis representing time and the vertical axis representing the actual inventory level. The semi-transparent areas of different colors correspond to the adaptively segmented time windows. It can be seen that the window contracts during peak promotional periods to capture rapid inventory changes, while it extends during stable periods to cover continuous trends. Overall, this indicates that the adaptive time window mechanism has a sensitive response to sudden inventory fluctuations and a function of local trend aggregation.

C. SPATIOTEMPORAL FUSION PREDICTOR BASED ON T-GCN

To extract the spatiotemporal dependency structure of inventory changes during promotions, synchronous input data (including time period sequences segmented from time windows and cross-platform adjacency matrices) were input into T-GCN [29,30]. The T-GCN computational framework consists of two parts: a graph convolution framework for handling cross-platform inventory dependencies and a gated loop framework for handling recursive processes at multiple consecutive time points, thereby enabling the input data to progressively eliminate node relationships within the time window and the recursion depth on the sequence trajectory. Sensor sequences generated after aligning and converting the time window to a fixed width were also used as the input basis for the graph convolutional layers. The cross-platform adjacency matrix was used to calculate weights and propagate them to all platforms, so that when drawing the graph, the sum of the increments generated by inventory changes could allow each node to receive these increment contributions when the inventory is updated. After the graph convolution is completed, the reverse state of the gated loop is used to recursively expand the forward and backward states of the time window. The state recursion does not depend on a fixed time span, but is performed sequentially according to the actual time steps within the window length. This ensures a high-density state flow during transition periods and a low update intensity during stable periods, thus forming a dynamic recursive trajectory consistent with the window rhythm. The model generates a spatiotemporally fused implicit representation at the output, which provides a continuous input for inventory forecasting at the next time step.

D. GRAPH CONVOLUTION AND NODE RELATIONSHIP PROPAGATION STRUCTURE

The graph convolutional layer uses a weighted adjacency matrix A as the core of the operation. It linearly combines the window input sequence Xt according to the node association strength, so that the inventory changes between platforms can form cross-node propagation during the convolution stage. The convolution calculation form is Formula 4:

$$H_t = \sigma(AX_tW) \tag{4}$$

W is the matrix to be trained, and $\sigma(\cdot)$ is the activation function. This structure is executed once at each time step, so that the cross-platform association is continuously updated within the entire window. The adjacency matrix comes from the graph construction process of the previous step. Therefore, the graph convolution carries information related to promotional events in the operation, so that nodes with high promotional response get higher weights in the propagation path, avoiding the occurrence of isolated nodes within the window [31,32]. The convolution output is the graph feature representation of each node at this time step. Its internal structure carries the trajectory of the influence of promotional events on inventory propagation, so that the inventory jump propagation path has a continuous expression in the feature dimension.

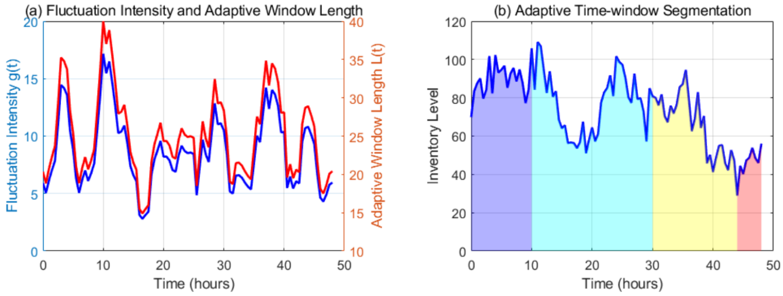

FIGURE 3. Results of adaptive time window rhythm extraction: (a) Changes in inventory fluctuation intensity and adaptive window length; (b) Inventory sequence division results of adaptive time window

E. TEMPORAL RECURSIVE MECHANISM OF GATED STRUCTURE

The graph convolution output sequence enters the gated loop structure in chronological order, forming a recursive chain of state variables within the window. The gated structure uses the node features after graph convolution as input, splitting state updates into two paths: an update gate and a reset gate. This allows the transition segments and gradual transition segments to form different response intensities during the temporal flow. The transition segment generates a larger update value due to the higher inventory change rate, allowing the state vector to more quickly approach the current inventory trend; the stable segment maintains a lower update due to the smaller change amplitude, preventing excessive fluctuations in the state [33,34]. This recursive structure, in conjunction with the adaptive window, ensures that local disturbances generated during the promotion phase are not weakened by other time periods, maintaining the complete transmission of the transition pattern within the temporal chain.

The recursive output forms a spatiotemporal fusion vector at the end of the window, which is recorded as a window-level feature and fed into the prediction layer. This allows the model to generate inventory prediction values in the final prediction stage based on cross-platform relationships and the internal rhythm of the window. This structure merges promotional rhythm, cross-node propagation, and window sequence patterns within the same framework, enabling inventory fluctuations during the promotional cycle to be mapped to the forecast input in a coherent manner, thus laying a continuous structure for cross-window forecasting.

III. PERFORMANCE VALIDATION STRUCTURE FOR INVENTORY FORECASTING DURING PROMOTIONAL PERIODS

The inventory forecasting experiment implements a set of operational records of natural fiber products from various sources. The experimentation utilizes real-world data from marketplace platform and service. The data has timestamps indicating when a product is promoted, when the product is in-stock or out-of-stock, and how many orders are placed for the products through each platform, as well as when there is a change in each platform's inventory. The data is divided by each promotional cycle; therefore, data from multiple consecutive promotional cycles contains stable segments. Out-of-stock days are removed, and abnormal replenishment points are removed to create the final usable sequence of data. The inventory data from each platform is collected at regular intervals typically ranging from minutes to hours. With this method, it is possible to capture quickly occurring changes for the purpose of forecasting inventory levels. Prior to conducting the experiment, data preparation is necessary to prepare for all missing points, to align all timestamps, to map all cross-platform nodes to ensure the differential trajectory is correct, and to ensure each dataset is captured at the same level of magnitude for input into the prediction algorithm. Due to the differences between promotional cycles with respect to duration, standardization of the time for comparison purposes are applicable. Based on the structure of the data and the fact that the data has been collected and aggregated into a continuous sequence for each of the promotional phases, the data can subsequently be evaluated with respect to several indicators such as error deviation, fluctuation-tracking sensitivity and multiplatform consistency deviation.

The original inventory data in this paper was collected with a minimum sampling interval of 5 minutes. To adapt to the model input and computational efficiency, we down-sampled the data at the hourly level during the preprocessing stage (taking the minimum inventory value per hour to retain the lower limit feature of "pulse"). Although the granularity is reduced, the adaptive window mechanism can still effectively respond to the sudden changes caused by promotions: on the one hand, the hourly data still contains significant fluctuations in promotion peaks; on the other hand, the window length adjustment is based on the smoothed first-order difference, which is robust to short-term pulses. This study provides a comparison of prediction errors under minute-level and hourly-level inputs. The results show that the difference in MAE is less than 0.3, indicating that downsampling does not significantly weaken the model's ability to capture pulse rhythms.

A. ERROR DISTRIBUTION DEVIATION VERIFICATION PROCESS

The error distribution deviation is based on the hourly difference between the predicted sequence and the actual inventory sequence, with the continuous trajectory of this difference constituting the error sequence. During evaluation, the error sequence is first smoothed to remove the influence of single-point spikes. Then, the concentration intervals and spans of the error during key promotional periods are statistically analyzed to determine the degree of deviation in the abrupt and gradual change phases of the prediction. The verification process starts with dividing the continuous error segments, grouping the positive and negative segments of the error, and aligning the deviation segments with the promotional nodes using the timestamps of the promotional phases as a reference. The duration of the deviation, the peak position of the deviation, and the range of deviation diffusion are recorded. A larger deviation indicates an unstable response of the prediction to the promotional rhythm; a smaller deviation indicates a better fit of the model's state updates during abrupt change phases.

The error behavior characteristics of inventory forecasting during promotional windows are assessed using Figure 4. Figure 4(a) shows the time series of errors, with the horizontal axis being the time point and the vertical axis being the forecasting error. The timeframes for promotional activity are denoted by green dashed lines. As seen in Figure 4(a), outliers of error are presented within multiple timeframe intervals, including 30-50, 90-100, and 150-170. This observation indicates that promotional activity has a greater impact on the statistical accuracy of the forecasting model. Additionally, the red smoothened line in Figure 4(a) illustrates that the outlier deviations are mostly contained in the promotional period. This determines the reference for subsequent testing of outliers. Figure 4(b) illustrates the rolling standard deviation index over the time points on the horizontal axis and the index of deviation on the vertical axis. Error instability is characterized by analyzing the rolling standard deviation of the error index. From that analysis, it is observed that there are multiple areas of high deviation occurring near the promotional periods, thus indicating that there are major structural disturbances in the inventory forecasting process due to promotional activity. This therefore indicates a need for both an adaptive rhythm-based model and a spatiotemporally based fusion process to suppress error propagation during promotional windows.

B. DETECTION STEPS FOR FLUCTUATION TRACKING SENSITIVITY

The ability of a model to track fluctuations is determined by analyzing the time it takes to produce a response to a jump point in the inventory prediction. The first step in this process is to identify where the jumps occur by extracting them from the actual inventory time series data (the input to the model) using the local extreme values from the inventory differential series as the jump criteria. Once a jump has been identified, the predicted value from the jump point is compared with the actual value from the jump point to determine the magnitude and direction of change in the predicted response (or rebound) as a result of the identified jump. Following this, the time delay between the predicted jump point and the actual jump point is calculated, and a statistical analysis of how well the model recoveries progress following the jump is conducted. The detection process occurs over several subintervals immediately adjacent to the jump segment, allowing for a complete assessment of the model's ability to follow very volatile promotional periods in which each customer's purchasing behavior is subject to frequent and sudden changes. Models that display greater sensitivity have a closer relationship between the jump segment update path and the warehousing rhythm, while those that do not have sufficient sensitivity display significant lag in their predicted rebound trajectory during the time immediately following the jump point.

Figure 5 illustrates the model's response to fluctuation signals when there are sudden jumps in the inventory series. In Figure 5(a), the horizontal axis represents time, and the vertical axis represents inventory level. The blue line represents the actual inventory series; the red line represents the predicted series; the green dots mark the jump points detected by the model. The series shows significant inventory jumps or decreases around times 30, 65, 100, 140, and 175, with the model's predicted curve showing a smaller lag compared to the actual curve. Figure 5(b) further magnifies the third jump point region, observing a rapid decrease in the actual inventory level near the jump point, while the predicted series shows a smaller response amplitude and a delay, indicating that the model's sensitivity to sudden fluctuations still has room for improvement.

C. COMPREHENSIVE PERFORMANCE COMPARISON WITH CONTROL MODELS

To verify the effectiveness of the prediction model integrating T-GCN and adaptive time window mechanism in the promotion cycle, this section selects four commonly used time series or graphical time series models as controls: LSTM (Long Short-Term Memory), GRU (Gated Recurrent Unit), T-GCN (without time window mechanism), and the traditional ARIMA (AutoRegressive Integrated Moving Average) model. Using multiplatform inventory sequences as input data, the average error indices, including MAE (Mean Absolute Error), RMSE (Root Mean Square Error), and Platform Consistency Index (CPI), are calculated for the pre-, mid-, and post-promotion periods. The stability of the models at transition points is also examined. To maintain a consistent evaluation dimension, all models use the same data partitioning and training parameters. Table 1 shows the advantages of the proposed T-GCN combined with an adaptive time window model in multi-platform promotional inventory forecasting. During the promotional period, ARIMA's MAE is 9.85; RMSE is 13.4; CPI is 0.42, showing slow response and poor cross-platform consistency. LSTM and GRU's MAE are 7.21 and 6.75, and CPI are 0.35 and 0.33, respectively, showing improved performance but still slow change response. The original T-GCN has an MAE of 6.10 and CPI of 0.29, with good cross-platform dependence but inaccurate capture of local mutations. The

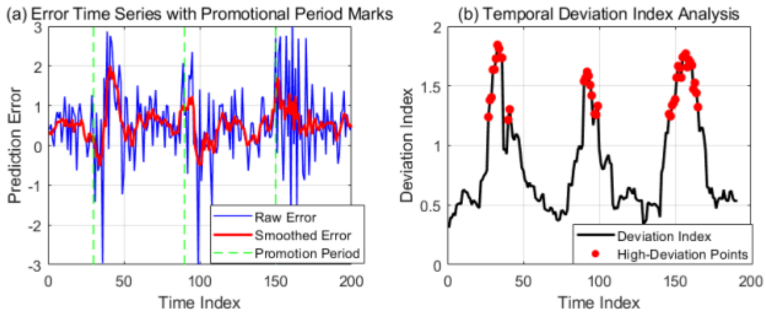

FIGURE 4. Deviation test flowchart for inventory forecasting errors during promotional periods: (a) Time series sequence of forecasting errors and promotional period markings; (b) Time series analysis of forecasting error deviation

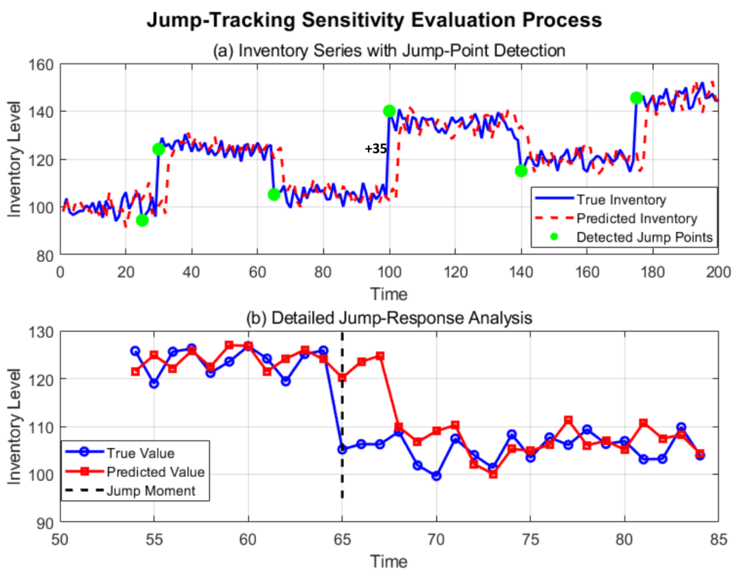

FIGURE 5. Predictive response performance of inventory series under fluctuation jumps: (a) Inventory series and jump point detection diagram; (b) Magnified analysis of jump point predictive response

proposed method reduces the MAE to 4.85, RMSE to 7.12, and CPI to only 0.18, with a two-step delay in change response, showing that the model significantly outperforms other methods in capturing sudden fluctuations and maintaining multi-platform consistency.

TABLE 1. Performance comparison of each model in inventory forecasting during the promotion cycle

Model	MAE (Pre-Promotion)	MAE (Promotion)	RMSE (Promotion)	CPI Platform Consistency ↓	Jump Point Response Delay (steps)
ARIMA	4.12	9.85	13.4	0.42	7
LSTM	3.05	7.21	10.32	0.35	5
GRU	2.98	6.75	9.8	0.33	4
T-GCN (Original)	2.65	6.1	9.05	0.29	4
Proposed Model	2.41	4.85	7.12	0.18	2

To more clearly separate the contributions of the adaptive time window mechanism and the T-GCN architecture, we added two control models in our experiments: "Time Window + LSTM" and "Time Window + GRU". These two models employ the same adaptive windowing strategy as the proposed method, only replacing T-GCN with LSTM or GRU for in-window sequence modeling. Results show that during the promotional period, the MAE of "Time Window + LSTM" is 6.32, and that of "Time Window + GRU" is 5.97, both outperforming the original LSTM/GRU (7.21/6.75), but still not reaching the performance of the proposed model (MAE=4.85). This indicates that the adaptive window mechanism itself has a gain effect, but the significant performance improvement still depends on T-GCN's explicit modeling ability for cross-platform graph structures.

IV. CONCLUSION

This paper focuses on the problem of predicting fluctuations in inventory levels for natural fiber products during the promotion periods of multi-platform e-commerce activities. A spatiotemporal forecasting framework is proposed that combines a T-GCN with a method for creating adaptive time windows. The first step of this study is to develop a cross-platform correlation graph of inventory levels and embed the research findings into an adjacency matrix, assigning weights to the connection between platforms based on the trend of inventory fluctuations and promotion rhythm during the promotional period. An adaptive time window is used to execute an accurate and timely slicing of the inventory time series to identify sudden changes in inventory level. The T-GCN is then utilized to capture both the time-series and graph structure characteristics of the inventory within each time window and to create window-by-window prediction vectors. The findings from the experiments indicate that this approach produces highly accurate inventory forecasts with low estimation errors during periods of significant promotion-driven inventory volatility, and a high degree of sensitivity in tracking fluctuations. Additionally, this approach reflects the complexities of cross-platform inventory synchronization. The limitations of this research include a delay in the response to unusual inventory fluctuations and limited prediction accuracy for specific promotional events. Future work includes integrating reinforcement learning-based techniques to refine the rules for adjusting time-window lengths and the exploration of more sophisticated graph structures for cross-platform inventory prediction to improve adaptability and generalizability.

AUTHOR CONTRIBUTIONS

Conceptualization – Junna Jin, Guiyu Fan, Jian Zhang and Xiaoyan Yu; methodology – Junna Jin, Guiyu Fan, Jian Zhang and Xiaoyan Yu; investigation – Junna Jin, Jian Zhang and Xiaoyan Yu; writing-original draft preparation – Junna Jin, Guiyu Fan, Jian Zhang and Xiaoyan Yu. All authors have read and agreed to the published version of the manuscript.

CONFLICTS OF INTEREST

The authors declare no conflict of interest.

FUNDING

This research was supported by Tangshan Social Sciences (TSSKL2024-124).

ACKNOWLEDGEMENTS

Not applicable.

REFERENCES

[1] J. Z. Zeng, A. Agarwal, and I. Stamatopoulos, "Promotional inventory displays: An empirical analysis using iot data," Manufacturing & Service Operations Management, vol. 26, no. 5, pp. 1826-1841, 2024, doi: 10.1287/msom.2022.0291.
[2] Z. Zeng, Y. Guo, Y. Ji, Y. Shi, and T. Feng, "Data-driven forecasting of pharmaceutical sales: distinguishing promotional vs," daily scenarios. International Journal of Data Mining and Bioinformatics, vol. 29, no. 5, pp. 1-26, 2025, doi: 10.1504/IJDMB.2025.147534.
[3] C. Li, W. Jiang, Y. Yang, S. Pan, G. Huang, and L. Guo, "Predicting best-selling new products in a major promotion campaign through graph convolutional networks," IEEE Transactions on Neural Networks and Learning Systems, vol. 34, no. 11, pp. 9102-9115, 2022, doi: 10.1109/TNNLS.2022.3155690.
[4] D. Kaul and R. Khurana, "Ai-driven optimization models for e-commerce supply chain operations: Demand prediction, inventory management, and delivery time reduction with cost efficiency considerations," International Journal of Social Analytics, vol. 7, no. 12, pp. 59-77. Retrieved from https://norislab.com/index.php/ijsa/article/view/104, 2022.
[5] R. Islam M and Z. Ikbal M, "Impact of predictive data modeling on business decision-making: A review of studies across retail, finance, and logistics," American Journal of Advanced Technology and Engineering Solutions, vol. 2, no. 2, pp. 33-62, 2022, doi: 10.63125/8hfbkt70.
[6] R. Karim M, "ARTIFICIAL INTELLIGENCE-ENHANCED PREDICTIVE ANALYTICS FOR DEMAND FORECASTING IN US RETAIL SUPPLY CHAINS," ASRC Procedia: Global Perspectives in Science and Scholarship, vol. 1, no. 1, pp. 959-993, 2025, doi: 10.63125/gbkf5c16.
[7] Y. Chen Z, P. Fan Z, and M. Sun, "Inventory management with multisource heterogeneous information: Roles of representation learning and information fusion," IEEE Transactions on Systems, Man, and Cybernetics: Systems, vol. 53, no. 9, pp. 5343-5355, 2023, doi: 10.1109/TSMC.2023.3267858.
[8] R. Liao and Y. Chai, "Research on the business performance evaluation method for small and medium-sized enterprises in cross-border e-commerce based on artificial bee colony optimized LSTM model," Scientific Reports, vol. 15, no. 1, pp. 316-398, 2025, doi: 10.1038/s41598-025-17435-x.
[9] Y. Xie, Q. Ye H, and W. Zhu, "Prediction and Optimization for Multi-Product Marketing Resource Allocation in Cross-Border E-Commerce," Journal of Theoretical and Applied Electronic Commerce Research, vol. 20, no. 2, pp. 124-126, 2025, doi: 10.3390/jtaer20020124.
[10] Y. Fu and M. Fisher, "The value of social media data in fashion forecasting," Manufacturing & Service Operations Management, vol. 25, no. 3, pp. 1136-1154, 2023, doi: 10.1287/msom.2023.1193.
[11] R. Singh, P. K. De, A. Barman, and P. Narang, "Optimal analysis of profit maximization production inventory system under an imperfect environment and shortage," OPSEARCH, no. 2, pp. 1-31, 2024, doi: 10.1007/s12597-024-00896-5.
[12] C. Cuartas and J. Aguilar, "Hybrid algorithm based on reinforcement learning for smart inventory management," Journal of intelligent manufacturing, vol. 34, no. 1, pp. 123-149, 2023, doi: 10.1007/s10845-022-01982-5.
[13] A. Paeizi, A. Makui, and M. S. Pishvaee, "A multi-stage stochastic programming approach for an inventory–routing problem considering life cycle," RAIRO-Operations Research, vol. 57, no. 5, pp. 2537-2559, 2023, doi: 10.1051/ro/2023122.
[14] M. Akter and S. P. Kudapa, "A Comparative Analysis of Artificial Intelligence-Integrated BI Dashboards For Real-Time Decision Support In Operations," International Journal of Scientific Interdisciplinary Research, vol. 5, no. 2, pp. 158-191, 2024, doi: 10.63125/47jjv310.
[15] R. P. Rooderkerk, N. DeHoratius, and A. Musalem, "The past, present, and future of retail analytics: Insights from a survey of academic research and interviews with practitioners," Production and Operations Management, vol. 31, no. 10, pp. 3727-3748, 2022, doi: 10.1111/poms.13811.
[16] H. K. Oh, H. Abdulla, and OlivaR, "Behavioral multi-lever decision-making: A study of consumer return policy, price, and inventory decisions," Journal of Operations Management, vol. 70, no. 1, pp. 137-156, 2024, doi: 10.1002/joom.1276.
[17] Z. Y. Chen, Z. P. Fan, and M. Sun, "Machine learning methods for data-driven demand estimation and assortment planning considering cross-selling and substitutions," INFORMS Journal on Computing, vol. 35, no. 1, pp. 158-177, 2023, doi: 10.1287/ijoc.2022.1251.
[18] M. R. Hasan, Y. Daryanto, C. Triki, and A. Elomri, "An inventory model of e-marketplace with a promotional program," Journal of Modelling in Management, vol. 19, no. 3, pp. 787-808, 2024, doi: 10.1108/JM2-01-2023-0011.
[19] A. R. Chowdhury, R. Paul, and F. Z. Rozony, "A systematic review of demand forecasting models for retail ecommerce enhancing accuracy in inventory and delivery planning," International Journal of Scientific Interdisciplinary Research, vol. 6, no. 1, pp. 01-27, 2025, doi: 10.63125/mbbfw637.
[20] H. Liu and X. Chen, "Rough approximation-based inventory optimization with random prices for B2C companies during the promotion period," International Journal of Intelligent Systems, vol. 37, no. 2, pp. 1408-1429, 2022, doi: 10.1002/int.22674.
[21] C. Zhang, X. Wang, C. Zhao, Y. Ren, T. Zhang, Z. Peng, et al., "Promotionlens: Inspecting promotion strategies of online e-commerce via visual analytics," IEEE Transactions on Visualization and Computer Graphics, vol. 29, no. 1, pp. 767-777, 2022, doi: 10.1109/TVCG.2022.3209440.
[22] A. Ridwan, U. Muzakir, and S. Nurhidayati, "Optimizing e-commerce inventory to prevent stock outs using the random forest algorithm approach," International Journal Software Engineering and Computer Science (IJSECS), vol. 4, no. 1, pp. 107-120, 2024, doi: 10.35870/ijsecs.v4i1.2326.

[23] K. Chaowai and P. Chutima, "Demand forecasting and ordering policy of fast-moving consumer Goods with promotional sales in a small trading firm," Engineering Journal, vol. 28, no. 4, pp. 21-40, 2024, doi: 10.4186/ej.2024.28.4.21.
[24] Y. Zhang, "Sales forecasting of promotion activities based on the cross-industry standard process for data mining of E-commerce promotional information and support vector regression," Journal of Computers, vol. 32, no. 1, pp. 212-225, 2021, doi: 10.4186/ej.2024.28.4.21.
[25] O. R. Amosu, P. Kumar, A. Fadina, Y. M. Ogunsuji, S. Oni, and K. Adetula, "Harnessing real-time data analytics for strategic customer insights in e-commerce and retail," World Journal of Advanced Research and Reviews, vol. 23, no. 2, pp. 880-889, 2024, doi: 10.30574/wjarr.2024.23.2.2407.
[26] K. K. Aggarwal and S. Ahmed, "Optimizing ordering, pricing and return strategies in an advanced sales inventory system with product screening," International Journal of System Assurance Engineering and Management, vol. 15, no. 12, pp. 5548-5573, 2024, doi: 10.1007/s13198-024-02524-3.
[27] O. R. Amosu, P. Kumar, Y. M. Ogunsuji, S. Oni, and O. Faworaja, "AI-driven demand forecasting: Enhancing inventory management and customer satisfaction," World Journal of Advanced Research and Reviews, vol. 23, no. 2, pp. 100-110, 2024, doi: 10.30574/wjarr.2024.23.2.2394.
[28] A. Hidayat, H. Susilowati, and A. Miranti, "Utilizing AI for Predicting Demand and Managing Supply Chains in Ecommerce Organizations," Journal of Management and Informatics, vol. 3, no. 2, pp. 250-266, 2024, doi: 10.51903/jmi.v3i2.32.
[29] J. Sun, Z. Wang, Z. Qiao, and X. Li, "Dynamic pricing model for e-commerce products based on DDQN," Journal of Comprehensive Business Administration Research, vol. 1, no. 3, pp. 171-178, 2024, doi: 10.47852/bonviewJCBAR42022770.
[30] Y. Hong, S. Sawang, and H. P. Yang, "How is entrepreneurial marketing shaped by E-commerce technology: a case study of Chinese pure-play e-retailers," International Journal of Entrepreneurial Behavior & Research, vol. 30, no. 2/3, pp. 609-631, 2024, doi: 10.1108/IJEBR-10-2022-0951.
[31] P. Broeder and E. Wentink, "Limited-time scarcity and competitive arousal in E-commerce," The International Review of Retail, Distribution and Consumer Research, vol. 32, no. 5, pp. 549-567, 2022, doi: 10.1080/09593969.2022.2098360.
[32] O. Ogunwole, E. C. Onukwulu, N. J. Sam-Bulya, M. O. Joel, and G. O. Achumie, "Optimizing automated pipelines for realtime data processing in digital media and e-commerce," International Journal of Multidisciplinary Research and Growth Evaluation, vol. 3, no. 1, pp. 112-120, 2022, doi: 10.54660/.IJMRGE.2022.3.1.112-120.
[33] S. Smerichevskyi, A. Kovalchuk, T. Obydiennova, S. Suvorova, V. Vlasova, and A. Tryvailo, "Development strategies for marketing and logistics in the innovative ecosystem of e-commerce," Revista Gestão & Tecnologia, vol. 25, no. 2, pp. 90-107, 2025, doi: 10.20397/2177-6652/2025.v25i2.3162.
[34] Y. Qi, X. Wang, M. Zhang, and Q. Wang, "Developing supply chain resilience through integration: An empirical study on an e-commerce platform," Journal of Operations Management, vol. 69, no. 3, pp. 477-496, 2023, doi: 10.1002/joom.1226.